GPS, COMMUNICATION AND ENVIRONMENTAL SENSOR BASED COLLISION MITIGATION SYSTEM FOR TRUCKS

Dipl.-Ing. Marc Wimmershoff
Institut für Kraftfahrzeuge Aachen (ika), RWTH Aachen University
Germany
Dipl.-Ing. Stefan Deutschle
Forschungsgesellschaft Kraftfahrwesen mbH Aachen (fka)
Germany

Paper Number 09-0070

ABSTRACT

In order to enable state of the art and future accident preventing systems (APS) to react appropriate in traffic situations, it is essential to monitor the driving environment. Therefore a new communication, GPS and environmental sensor based method for APS data acquisition was developed. This method uses GPS, vehicle related driving dynamics data, wireless car-2-car-communication (C2C) and combines them with on-board environmental sensor data (Camera and Lidar sensors).
First a Kalman-Filter based GPS-tracking was developed in order to increase the update rate of GPS. Therefore GPS- and vehicle dynamics data are fused in a dead reckoning system. Second, a Kalman-Filter based 3rd order lane model was implemented using Camera data from ego- and preceding vehicle - transmitted by C2C - for the determination of the relevant target. Beyond vehicle related data are transferred from the target vehicle to the ego-vehicle in order to improve the target selection. The potential of this method was demonstrated in a prototype collision mitigation (CM) system. The system was tested within driving experiments and subsequent simulations with the measured data.
With the new method the accuracy and scope of application of collision mitigation systems can be enhanced, so that the detection and identification of stationary vehicles, for example at the end of traffic jams, is improved. Furthermore a high reliability of the determination of the relevant target for APS can be reached.
As a matter of course the limitation of this approach is the dependency of the system performance (as in all C2C and environmental sensor based systems) on the equipment rate. On the other hand it can be expected that equipment rates will increase in future.

INTRODUCTION

Regarding commercial vehicles, rear-end collisions count among the most frequent occurring accident types [1]. Especially rear-end collisions with high relative velocities are dangerous if commercial vehicles are involved because of their high mass. The GIDAS data base (**G**erman **i**n-**D**epth **A**ccident **S**tudy) shows that car drivers perform an emergency stop (6 m/s² to 10 m/s²) only in 22 % of all accidents. In approximately 78 % of the collisions an insufficient deceleration (0 m/s² to 6 m/s²) is executed [2]. [3] points out that nearly 60 % of all rear-end collisions and almost one third of all head-on collisions - the correct reaction assumed - could be avoided, if the driver would react half a second earlier. These values show the potential of advanced driver assistance systems (ADAS) supporting the vehicle longitudinal dynamics.
Nowadays, there are already brake assists in series production, initiating an emergency stop, if a collision with a vehicle driving in front seems unavoidable. Further systems are under development. Today, Radar and Lidar sensors as well as Camera systems are the basis for the detection of an imminent collision. Out of this an abundance of challenges arise, for example the recognition of an object standing still or the misinterpretation of warning beacons at motorway constsruction sites. Present series systems only react on moving objects or objects, which were in motion at the beginning of the detection. Within this paper an approach is described that uses the GPS position and further data of the preceding vehicle, all transmitted by C2C to allow a detection of stationary target objects.
This paper is structured as follows: first the Kalman-Filter based models are introduced. On the one hand an Extended Kalman-Filter (EKF) based ve-

hicle model (GPS-Tracking) calculating global positioning data between two GPS data updates is implemented. With the help of this GPS-Tracking and a C2C a position measurement is employed. On the other hand a Kalman-Filter based street model is implemented that uses data measured by ego- and preceding vehicle. The street data from the preceding vehicle is also transmitted by C2C. The next chapter deals with the used hardware. It contains the description of the test vehicles, sensors, C2C, GPS receiver and the utilised computation hardware. Afterwards an overview of the system architecture is given. In the last chapter the results of test drives in real traffic, on the test track and the results of simulations with measured data are presented.

KALMAN-FILTER BASED VEHICLE- AND STREET MODELLING

The vehicle- and the street model describe the current condition of the vehicle and the environment. The state estimation of the model is supported by a Kalman-Filter.
In a first step a vehicle model is developed, which describes the dynamic movement of the vehicle in Gauß-Krüger (GK) coordinates. In a second step the road is modelled, in order to describe the movements of the host vehicle in the lane and generate a path prediction. Both models are based on state space description. In the following the models and their mathematical formulation are presented.

Vehicle Model (GPS-Tracking)

The vehicle model describes the position and direction of motion (course) of the vehicle in GK coordinates. Therefore a mass point, moving in the GK coordinate system, is considered (Figure 1). With the GPS data and the subsequent GK coordinate transformation, the x- and y-coordinates of the vehicle (x_{GK} and y_{GK} in Figure 1) are described with the GPS update frequency of 1 Hz. Furthermore, the course angle τ is given, which is also included in the GPS data. If a speed of 80 kph is assumed for commercial vehicles on motorways, then the vehicle travels 22,22 m within the GPS update rate. Since a GPS based positioning system should be realised, it is necessary to have a higher positioning update of the host vehicle (> 1 Hz). This is realised in an EKF based vehicle model, delivering additional position information between two GPS measurements.
As shown in Figure 1, the course angle τ has a value of 0° if the vehicle moves into north direction. Furthermore, the positive rotation direction of τ is clockwise while the positive rotation direction of the vehicle yaw rate $\dot{\psi}$ is counterclockwise. Beyond the yaw angle ψ_{GPS} is defined to be the angle between the y-coordinate of the GK coordinate system and the vehicle's longitudinal central axis.

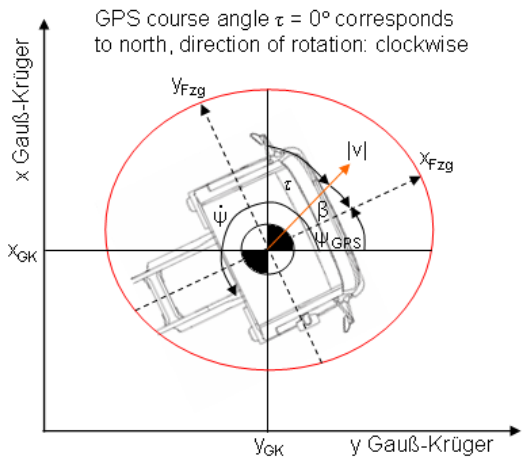

Figure 1. Angles in GK coordinate system.

Modelling the mass point's motion in the GK coordinate system can be done on different complexity levels. Within the object modelling two different models are commonly used, the model of constant acceleration or the model of constant velocity.
The model of constant acceleration takes the position, the velocity and the acceleration of the vehicle into account, see Equation (1).

$$p_{k+1} = p_k + v_k \cdot \Delta t + a_k \cdot \frac{\Delta t^2}{2} \qquad (1).$$

The model of constant velocity is a simplification of the model of constant acceleration by leaving out the acceleration term. Thus, Equation (1) is simplifyed to Equation (2).

$$p_{k+1} = p_k + v_k \cdot \Delta t \qquad (2).$$

The movement of the object is described separately in longitudinal- and in lateral direction. Independently which object model is choosed, the state vector **x** for the vehicle model is given by:

$$\mathbf{x} = [x_{GK} \quad y_{GK} \quad \psi_{GPS}]^T \qquad (3).$$

It includes the position of the vehicle in x- and y-direction in the GK coordinate system and the yaw angel ψ_{GPS}. In this paper, the model of constant velocity was chosen as the motion of commercial vehicles (especially on highways) is very steady. For future works the implementation of a constant acceleration model in combination with a multiple model adaptive estimator (MMAE) is planned.
With the model of constant velocity, the discrete model equations for the Kalman filter can be de-

termined. Under consideration of the slip angle β and $v_k \cdot \Delta t$ replaced with Δx_k Equation (4) is valid.

$$\begin{bmatrix} x_{GK,k+1} \\ y_{GK,k+1} \\ \psi_{GPS,k+1} \end{bmatrix} = \begin{bmatrix} x_{GK,k} \\ y_{GK,k} \\ \psi_{GPS,k} \end{bmatrix} + \begin{bmatrix} \Delta x_k \cos\beta_k \sin\psi_{GPS,k} + \Delta x_k \sin\beta_k \cos\psi_{GPS,k} \\ \Delta x_k \cos\beta_k \cos\psi_{GPS,k} + \Delta x_k \sin\beta_k \sin\psi_{GPS,k} \\ \dot{\psi}_k \Delta t \end{bmatrix} \quad (4)$$

A visualisation of the state equations is given in Figure 2. Because of the included trigonometric functions, an extended Kalman-Filter must be used.

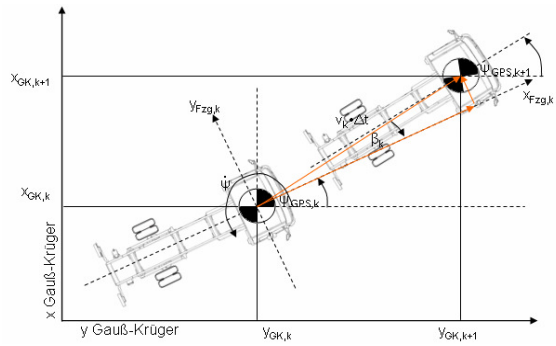

Figure 2. GPS vehicle motion model.

The measurement vector **y** is equal to the state vector. Hence the measurement matrix **C** for the vehicle model is given by a 3x3 identity matrix.

Street Model

For a better understanding the variables used within the street model are introduced according to Figure 3. These are the lateral position of the vehicle in lane (y_0) related to the centre of the lane and the relative yaw angle ψ_{lane}, showing the orientation of the vehicle in the lane, see Figure 3.

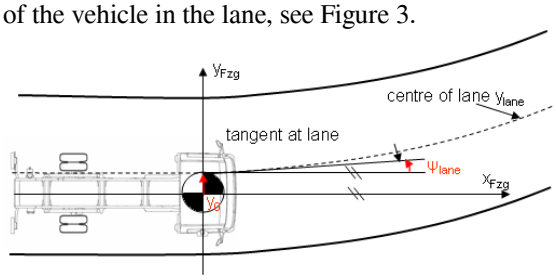

Figure 3. Lane model and variables [4].

Generally, the trajectory of the street can be composed of several routing segments, describing a sequence of straight and curved parts. Since the transition from a straight part into a curve with constant radius would mean a sudden step in the road curvature, the transition elements of roads are build as clothoids [5].

Modelling – The street model uses a 3rd order polynom according to [4]:

$$y_{lane}(x_{Fzg}) = y_0 + \psi_{lane} x_{Fzg} + \frac{C_o}{2} x_{Fzg}^2 + \frac{C_1}{6} x_{Fzg}^3 \quad (5).$$

This equation describes the trajectory of the lane as a function of the vehicle longitudinal axis. Based on the parameters, needed for the trajectory estimation, the state vector can be derived. Doing so, the lane offset y_0, the orientation of the vehicle ψ_{lane}, the curvature C_0, the change of curvature C_1 and the lane width B are state variables of the model.

$$\mathbf{x} = [y_0 \quad \psi_{lane} \quad C_0 \quad C_1 \quad B]^T \quad (6).$$

Using discrete time steps t_k for the lane offset $y_{0,k}$, Figure 4 shows that the following equation is valid:

$$y_{0,k+1} + \Delta y_{Fzg,k} = y_{0,k} + \Delta y_{lane,k} \quad (7).$$

The lane offset of the next time step $y_{0,k+1}$ is thus calculated by the sum of the current lateral lane offset $y_{0,k}$ and the change of the y-coordinate due to the lane curvature ($\Delta y_{lane,k}$), minus the change of the y-coordinate due to yaw movement ($\Delta y_{Fzg,k}$):

$$\Delta y_{lane,k} = \psi_{lane,k} v_k \Delta t + \frac{C_{o,k}}{2}(v_k \Delta t)^2 + \frac{C_{1,k}}{6}(v_k \Delta t)^3 \quad (8).$$

$$\Delta y_{Fzg,k} = v_k \Delta t \sin(\dot{\psi}_k \Delta t) \approx v_k \dot{\psi}_k \Delta t^2 \quad (9).$$

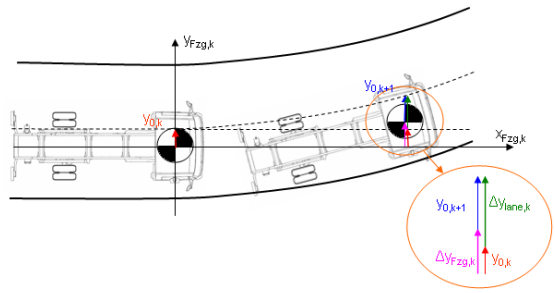

Figure 4. Lateral position in lane.

Comparable to the lateral position in lane the angle $\psi_{lane,k+1}$ can be calculated from the sum of $\psi_{lane,k}$ and the change of the angle $\Delta\psi_{lane,k}$ minus the vehicle motion $\Delta\psi_{Fzg,k}$.

$$\psi_{lane,k+1} + \Delta\psi_{Fzg,k} = \psi_{lane,k} + \Delta\psi_{lane,k} \quad (10).$$

$\Delta\psi_{lane,k}$ is equal to the gradient angle of the road at the position $x_{Fzg,k} = v_k \cdot \Delta t$. The gradient angle of a straight line is defined as follows:

$$\alpha = \arctan\left(\frac{\Delta y}{\Delta x}\right) \approx \frac{\Delta y}{\Delta x} = \frac{dy(x)}{dx} \qquad (11).$$

Using a small angle approximation ($\tan \alpha \approx \alpha$) it is possible to replace the gradient angle α by the gradient value of the straight line. Transferred to the course of the road (no consideration of the ego-lane angle is necessary), the angle $\Delta\psi_{lane,k}$ is equal to the first derivation of the lane equation (5).

$$\Delta\psi_{lane,k} \approx C_{o,k} v_k \cdot \Delta t + \frac{C_{1,k}}{2}(v_k \cdot \Delta t)^2 \qquad (12).$$

Furthermore, the yaw angle during the timeframe Δt ($\Delta\psi_{Fzg,k}$), can be expressed as follows:

$$\Delta\psi_{Fzg,k} = \dot{\psi}_k \cdot \Delta t \qquad (13).$$

In order to discretise the current curvature C_0, the second derivation of (5) respectively the third derivation for the change of curvature C_1 can be used.

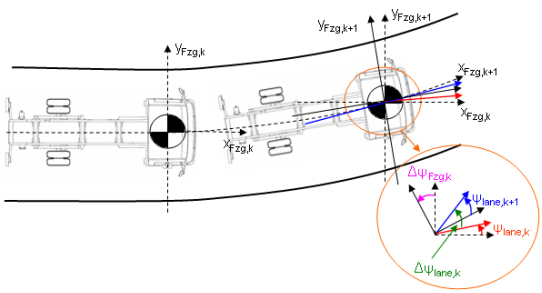

Figure 5. Relative yaw angle in lane.

By using discrete points of time for observation, the matrixes needed for the Kalman-Filter are gained with the help of the equations mentioned above. For a better reading the term $v_k \cdot \Delta t$ is substituted by Δx. Thus, the system matrix **A** is given as follows:

$$\mathbf{A} = \begin{bmatrix} 1 & \Delta x & \Delta x^2/2 & \Delta x^3/6 & 0 \\ 0 & 1 & \Delta x & \Delta x^2/2 & 0 \\ 0 & 0 & 1 & \Delta x & 0 \\ 0 & 0 & 0 & 1 & 0 \\ 0 & 0 & 0 & 0 & 1 \end{bmatrix} \qquad (14).$$

The input matrix **B** takes the yaw rate $\dot{\psi}_k$ and the velocity v_k of the vehicle into account.

$$\mathbf{B} = \begin{bmatrix} -v_k \cdot \dot{\psi}_k \cdot \Delta t^2 & -\dot{\psi}_k \cdot \Delta t & 0 & 0 & 0 \end{bmatrix}^T \qquad (15).$$

The measurement matrix **C** has to be adapted individually to the sensor and the communication.

USED HARDWARE

Having described the development of the vehicle model and the street model in the previous section, this chapter deals with the used hardware.
For the development and testing of commercial vehicle ADAS, two experimental trucks are available at ika (Institut für Kraftfahrzeuge, RWTH Aachen University). One is an IVECO Stralis AS 440 S 48 T/P EURO 3 with a 16-speed automatic gearbox (Figure 6). The second truck is an IVECO Stralis AS 440 S 48 T/P EURO 5 anticipo with a 12-speed automatic gearbox. Both vehicles are equipped with 367 kW engines, hydrodynamic retarder and WABCO Adaptive Cruise Control. The vehicles' steering is automated with ZF ServoTwin Steering Actuators (torque super position) and the longitudinal dynamic is automated with a WABCO acceleration interface. Thus an external steering and acceleration/braking via CAN bus enabled.
Figure 6 shows one IVECO test truck with the used environmental sensors: a monocular HELLA Camera and HELLA IDIS Lidar sensor. The Camera system is equiped with an algorithm for lane- and vehicle detection and delivers data about surrounding vehicles and the trajectory of the road. The road trajectory data are curvature $C_{0,CAM}$, lane width B_{CAM} and lateral lane offset $y_{0,CAM}$ (compare Figure 7). Beyond, the truck is equipped with a DENSO lane recognition camera, a 77 GHz WABCO Radar sensor and two 24 GHz HELLA Radar Near Distance Sensors (NDS).

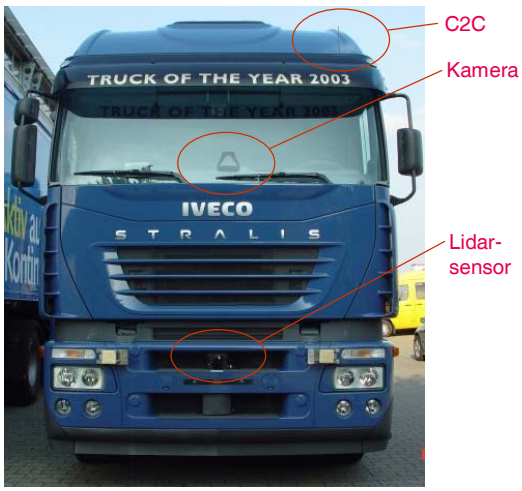

Figure 6. One of ika's experimental trucks.

In order to enable a wireless communication between the two trucks, WIRELESS CAN boxes

(called WCAN) by Agilion are installed in the trucks. The WCAN boxes allow a wireless connection between two or more network participants and are based on the robust radio technology nanoNET, a wide band communication technology in the 5.8 GHz band.

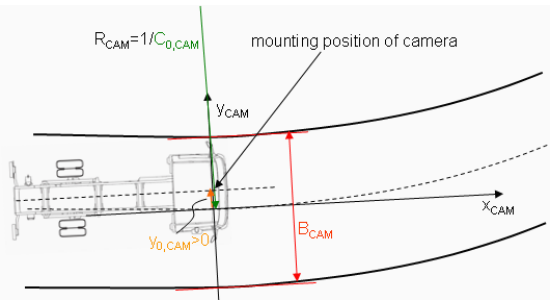

Figure 7. Data delivered from HELLA camera.

The GPS receivers used in this work are the GNS 5843 receiver from GNS, Global Navigation Systems company. GNS 5843 is a GPS-RDS/TMC-receiver with a Sirf-III chipset, supporting the NMEA 0183 data protocol. The cycle time is one second.
The target hardware for the developed system is the dSPACE Autobox for rapid prototyping experiments which offers the possibility of testing real-time software on-bord. The software is developed with Matlab/Simulink and compiled with Real Time Workshop for the Autobox.

SYSTEM ARCHITECTURE

Our communication and environmental sensor based CM system for trucks needs robust data from the ego-vehicle and the environment. Therefore it is necessary to employ a GPS-tracking, that calculates the current position of the vehicle in the GK coordinates. By means of the wireless communication, the GK coordinates and other vehicle relevant signals of a preceding vehicle are received in the following vehile. In combination with the IDIS Lidar sensor data, the received wireless data is combined and delivers a relevant target. Furthermore, the trajectory of the lane is predicted and is available for the CM system.
In the following, the system architecture and modules are described.

Architecture – Figure 8 shows the architecture of the system. The measurement data are either used for determinatoin of the relevant target or delivered to the vehicle- or street model.
GPS and vehicle sensors deliver measurement data to the vehicle model, executed each 10 ms. By means of an EKF, a GPS-tracking is built, providing position data of the vehicle in GK coordinates.
The Camera system and the vehicle sensors deliver measurement data to the Kalman-Filter based street model and a robust prediction of the lane trajectory is reached. The street model is triggered with camera measurement data (cycle time 50 ms).
With the help of the IDIS Lidar sensor and the data gained by C2C, the relevant target vehicle is determined. A relevant target can only be present, if the target vehicle and the ego-vehicle drive in the same lane. In this case, the lane trajectory runs through the target vehicle and a correction of the lane trajectory with the help of the relative coordinates of the target vehicle can be performed.
The architecture shown in Figure 8 is for implementation divided into five modules: the GPS modul, WLAN modul, vehicle data model, environmental modul and CM modul.

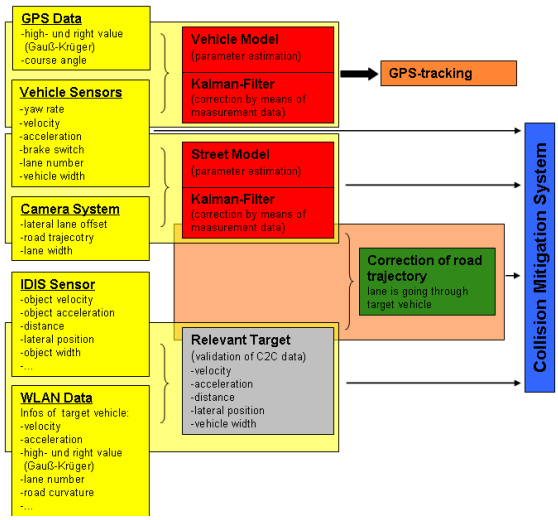

Figure 8. CM system architecture.

The GPS modul constains the vehicle model with GPS-tracking while the WLAN modul contains the transmission and receiving of the wireless messages. The vehicle modul is responsible to deliver the vehicle relevant data from CAN bus. The environmental modul contains the algorithm for the determination of the relevant target and the street model. The CM modul consists of the CM system.

Vehicle Data Modul – The vehicle data modul delivers the relevant vehicle data from CAN bus and provides these data for further processing. In detail, these data are the yaw rate $\dot{\psi}_{ego}$, the vehicle velocity v_{ego} and the brake switch flag. The vehicle acceleration in longitudinal direction a_{ego} is gained from the velocity by a Luenberger observer [6].
Further signals, generated within the vehicle data modul, are the vehicle width and the lane number. The vehicle width is hard coded with the width of the test vehicle (2.55 m). The lane number is defined as shown on Figure 9.
Up to now, no algorithm for the lane number determination is implemented, thus the lane number for the performed tests was also hard coded.

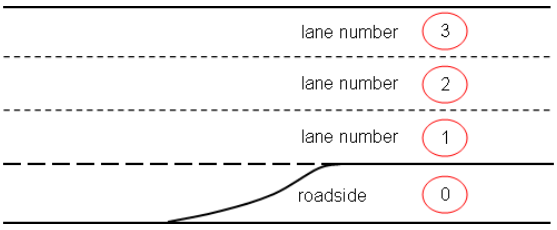

Figure 9. Definition of lane numbers.

GPS Modul – The GPS Modul contains the GPS-tracking. The GPS-tracking first transforms the GPS position (latitude, longitude and height) into the GK coordinates followed by generation of the measurement vector $\mathbf{y}_{GPS}$. The course angle τ has to be converted (16). Up to now, the slip angle β is not used in the test vehicle, but as the CM system is designed for highways the slip angle can be neglegted and (16) is simplified to (17):

$$\psi_{GPS} = 90° - \tau - \beta \qquad (16).$$

$$\psi_{GPS} \approx 90° - \tau \qquad (17).$$

Hence, the state equations of the vehicle model are:

$$\begin{bmatrix} x_{GK,k+1} \\ y_{GK,k+1} \\ \psi_{GPS,k+1} \end{bmatrix} \approx \begin{bmatrix} x_{GK,k} \\ y_{GK,k} \\ \psi_{GPS,k} \end{bmatrix} + \begin{bmatrix} \Delta x \cdot \sin\psi_{GPS,k} \\ \Delta x \cdot \cos\psi_{GPS,k} \\ \Delta t \cdot \dot{\psi}_k \end{bmatrix} \qquad (18).$$

The measurement vector can be written with the current GK coordinates respectively the yaw angle and is available for the vehicle model.
The input data of the GPS-tracking are the yaw rate and the velocity of the vehicle. For the EKF, the state equations are differentiated with respect to the state vector **x** to obtain the matrix **A**:

$$\mathbf{A} = \begin{bmatrix} 1 & 0 & \Delta x \cdot \cos\psi_{GPS,k} \\ 0 & 1 & -\Delta x \cdot \sin\psi_{GPS,k} \\ 0 & 0 & 1 \end{bmatrix} \qquad (19).$$

Since an GPS update (cycle time 1 s) occurs not in each time step of the vehicle model (cycle time 10 ms), the innovation of the EKF is set to zero, if no GPS update occurred. In this case the state variables of the vehicle model are updated only based on the model itself.

WLAN Modul – The WLAN modul receives and transmits data via C2C. The modul of the target vehicle transmits the relevant data while the modul of the ego-vehicle receives data. Transferred data are: velocity, longitudinal acceleration, yaw rate, brake switch, lane number, vehicle width, GK coordinates, lateral position in lane and curvature.
Velocity, longitudinal acceleration, yaw rate, brake switch, lane number and vehicle width are taken from the vehicle data modul while the lateral position in lane and the road curvature are obtained by the environmental modul. The GK coordinates are converted to the coordinates of the truck's rear end. By means of the GK positioning data of the target vehicle's rear and the ego GK positioning data, the relative location of the target vehicle with respect to the ego-vehicle can be calculated, see Figure 10. Therefore, the angle α_{target} is determined:

$$\alpha_{target} = \arctan\left(\frac{x_{GK,target} - x_{GK,ego}}{y_{GK,target} - y_{GK,ego}}\right) - \psi_{GPS,ego} \qquad (20).$$

With the help of α_{target} the relative position of the target vehicle dx_{GPS} und dy_{GPS} can be calculated:

$$dx_{GPS} = \sqrt{(x_{GK,target} - x_{GK,ego}) + (y_{GK,target} - y_{GK,ego})} \cdot \cos\alpha_{target} \qquad (21).$$

$$dy_{GPS} = \sqrt{(x_{GK,target} - x_{GK,ego}) + (y_{GK,target} - y_{GK,ego})} \cdot \sin\alpha_{target} \qquad (22).$$

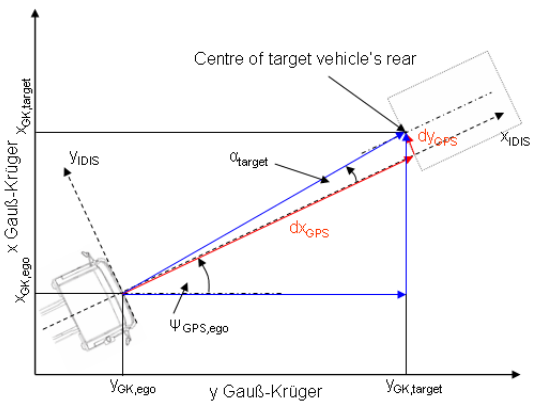

Figure 10. Determination of the target vehicle's relative position.

Environmental Modul – The environmental modul differs for the ego- and target vehicle. The target vehicle modul consists only of camera data input to transmit them to the ego-vehicle via C2C.
The environmental modul of the ego-vehicle contains the input of the camera data, the input of the IDIS Lidar sensor and an algorithm comparing the IDIS data with the positioning data gained by C2C. Furthermore, the street model is implemented in the environmental modul.
The determination of potential target vehicles consist of the evaluation of the following attributes:

- Object data declared as valid by the sensor
- Distance is less than 100 m
- Object width less than lane width

Furthermore, each IDIS object has a lifetime counter. Having checked these attributes, a list of potential target vehicles is available. The next step for the determination of the target vehicle is depicted in Figure 11. Here, the redundant object data

(from C2C and IDIS sensor) are compared. These are the relative object position in x- and y-direction, the velocity, width and acceleration of the target vehicle. For all potential target vehicles the absolute signal difference from IDIS- and C2C data are calculated. For the differences thresholds are defined within the algorithm. If any signal difference is higher than the threshold, the IDIS object is not regarded as target vehicle.

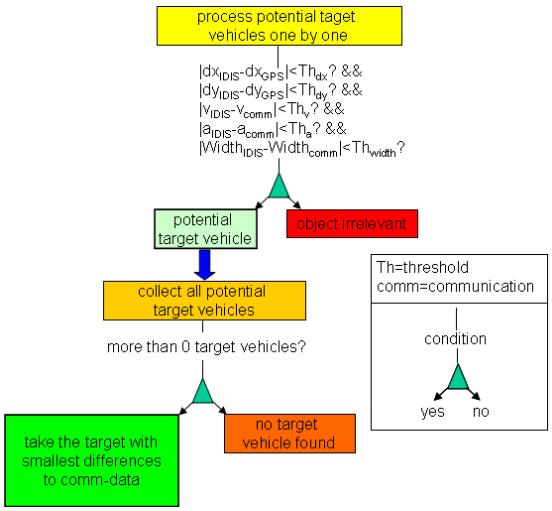

Figure 11. Determination of target vehicle.

In case of having more than one IDIS object after this procedure, the algorithm regards that object to be the target vehicle, whose sum of all signal differences is smallest.

The implementation of the street model is also part of the environmental modul in the ego-vehicle. The input signals are the data measured by the camera in the ego-vehicle and the curvature measured by the Camera of the target vehicle, transmitted to the ego vehicle ($C_{0,CAM,target}$). With the knowledge of $C_{0,CAM,target}$ the change of roard curvature is:

$$C_1 = \frac{C_{0,target} - C_{0,ego}}{dx_{target}} \quad (23).$$

The value dx_{target} describes the distance of the target vehicle in longitudinal direction. The measurement vector $\mathbf{y}_{lane}$ of the street model is now given by:

$$\mathbf{y}_{lane} = [y_{0,CAM,ego}\ C_{0,CAM,ego}\ C_{0,CAM,target}\ B_{CAM,ego}]^T \quad (24).$$

The output of the Kalman-Filter is the state vector. This signal passes a further function that corrects the state variables $C_{0,ego}$ and $C_{1,ego}$ in case of an existing target vehicle. Is this the case, it is ensured that the ego- and target vehicle drive in the same lane. With the knowledge of the lateral lane offset $y_{0,CAM,target}$ and the position of the target vehicle (dx_{target}, dy_{target}) the curvature $C^*_{0,ego}$ can be calculated by neglecting the change of curvature C_1:

$$dy_{target} - y_{0,CAM,target} = y_{0,ego} + \psi_{lane,ego} dx_{target} + \frac{C_{o,ego}}{2} dx_{target}^2 + \frac{C_1}{6} dx_{target}^3 \quad (25).$$

$$C^*_{o,ego} = \frac{2\left(dy_{target} - y_{0,CAM,target} - y_{0,ego} - \psi_{lane,ego} \cdot dx_{target}\right)}{dx_{target}^2} \quad (26).$$

EXPERIMENTS AND RESULTS

The developed models are tested in different test drives. While driving, measurement data of the sensors, communication and model data are recorded in the ego-vehicle. The recorded data are later used as input for simulations in Matlab/Simulink. Thus, the model parameter can be modified and the effect can be evaluated.

For tuning of the GPS-tracking, test drives without target vehicle are executed. In order to examine the functionality of the street model and to give a statement about the C2C and GPS based position measurement accuracy, test drives with two test vehicles are executed. The test drives are carried out at different velocities on straight and curved roads and on a test track with a static target vehicle and the ego-vehicle approaching at different velocities.

Function check and tuning of GPS-tracking

The first manoeuvre for the function check of the GPS-tracking is a steady-state circle drive. Six tests are carried out, clockwise and three counterclockwise on a diameter of 80 m and 40 m. The tests on the 80 m diameter are done with a velocity of 25 kph and 40 kph while the tests on the 40 m diameter are done with 25 kph. An evaluation of a test on the 80 m circle with 25 kph before and after filter tuning is depicted in Figure 12.

In the lower diagram of Figure 12 it can be seen that the model behaviour after the filter tuning delivers better results. The evaluation of the test drive delivers a diameter of 80.35 m (corresponds to a difference of 0.35 m). If all tests are taken into account, the maximum difference for the 80 m circle is 2.5 m and for the 40 m circle 2 m.

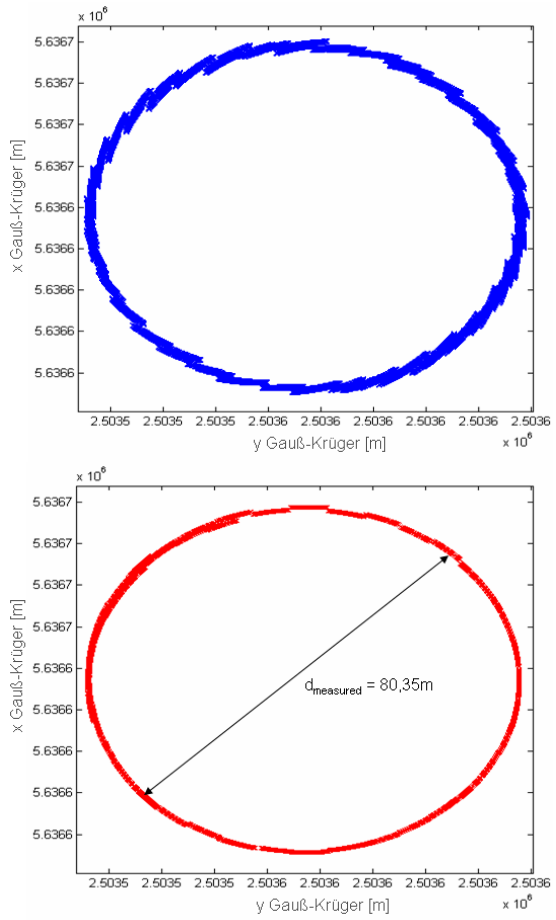

Figure 12. Results of GPS-tracking before (above) and after filter tuning (below).

Despite the filter tuning the circle in the lower diagram of Figure 12 shows steps in the signal due to GPS data update. Between two GPS data updates the GK coordinates and the course angle are updated model based. The evaluation of the tests with tuned filter parameters shows that the maximum difference between the new received GPS position and the model based position is less than 1.5 m. Thus, it can be stated that the vehicle model delivers valid data. To ensure that the vehicle model delivers not only in steady-state scenarios valid data, test drives in real traffic are executed.

Here the GPS- and vehicle data were also recorded for later offline simulations and the result is shown in Figure 13.

The track contains straight parts and also curves with large and small radii. Hence, it is well used to examine the model function and perform a filter tuning. In Figure 13 red and blue position plots are given. The blue plots show the GPS measurement data from the receivers. The red plots are the tracked coordinates after further filter tuning.

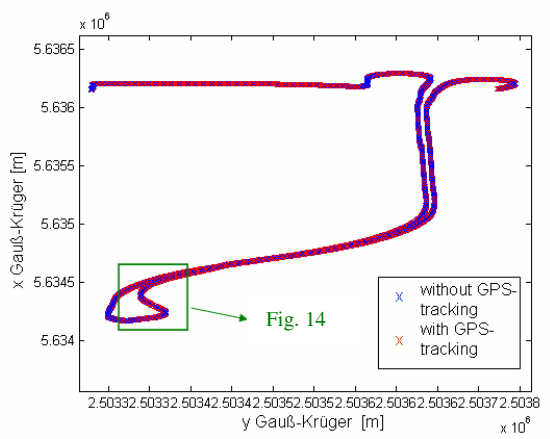

Figure 13. Measurement on real road.

Figure 14 shows a detail from the track (green in Figure 13). The model is doing well on straight and curved parts with a slight tendency to less accuracy for increasing curvature. The course angle τ is on the one hand less accurate during a change of motion direction and on the other hand time-delayed. Furthermore, the side slip angle β is neglected, which is correct for highway driving conditions but leads to mistakes on narrow curves. Hence, using a receiver with a better course angle and implementing a slip angle estimator could increase the results.

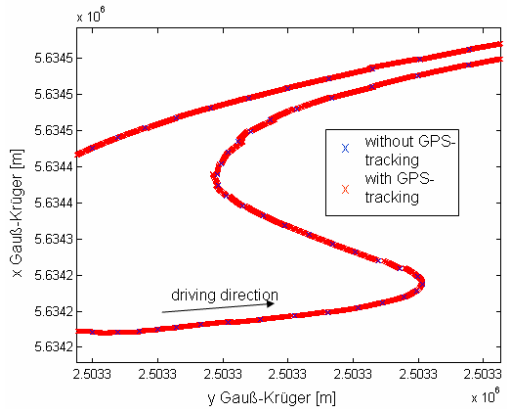

Figure 14. Extract of measurement.

As a further factor the traction and brake slip influences the performance. During strong acceleration and deceleration a higher difference between new measured and estimated position was found. In order to remove this influence, a reference velocity should be used in future, weighting the front axle speed sensors more during acceleration and rear axle speed sensors more during deceleration. Within all tests the largest difference between measured and estimated position was 2.51 m with an average value of 0.57 m after filter tuning.

Function check and tuning of street model

Comparable to the functional check of the vehicle model, driving tests were performed for testing and filter tuning of the street model.
In total 30 test runs were done for the functional check, ⅓ on straight roads, ⅓ on positive curvature (left turn) and ⅓ on negative curvature (right turn), with velocities between 60 to 90 kph. For the later offline simulations and tuning of the street model, again all relevant data were recorderd. Tuning of the object plausibility check algorithm is described in a later section, the simulation results of the street model are described now.
Figure 15 shows the lateral position in lane for a test drive on a straight road. The measurement data are marked blue and the model data red.
At the beginning, the Kalman-Filter needs some time to engage (Figure 15). Regarding the measured position in lane, at 12 s one can see a dropout. The sensor system did not detect the lane correctly, but the street model delivers a steady signal and is not influenced by this dropout.

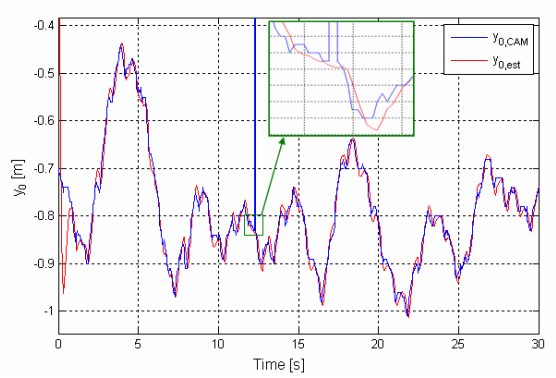

Figure 15. Measured and estimated position.

Figure 16 shows the results for the lane width of the same run. Here one can also find the dropout in the blue measurement data at 12 s and again the model based red signal is stable and not influenced. The lane width delivers correct values between 3.6 and 3.8 m which are in the range of values defined for German highways (3.75 m according to [5]).
In order to give a statement about the quality of the curvature and curvature change signal, the tests on curved roads are used. The test track is the last part of the highway A544 in Aachen, shown in Figure 17 (marked blue). The test track is driven in both directions in order to get data of right-hand- (negative curvature) and left-hand bend (positive curvature). With the help of a satellite picture and GPS data, a reference value for the radius of this curve was determined to 600 m (curvature 0.00167 m^{-1}).
The test drives were done with 60 and 90 kph and different distances (varying from 15 to 100 m) between the trucks in order to evaluate distance influences on the result.

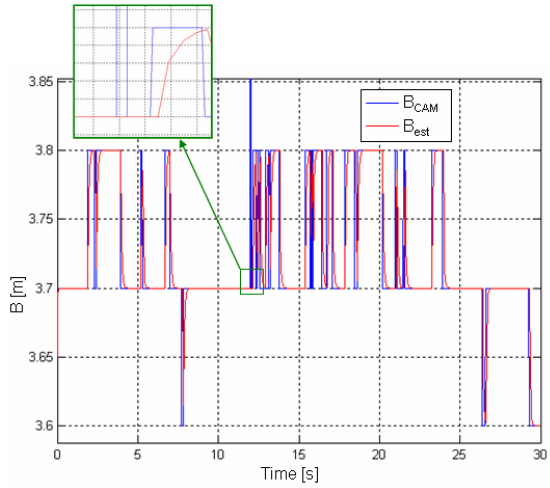

Figure 16. Measured and estimated lane width.

The evaluation of one measurement is shown in Figure 18. Because of the driving direction, positive curvature values should occur (direction 2, see Figure 17). Again the measurement data are marked blue, model data are marked red and the filter needs some time to engage on the beginning.

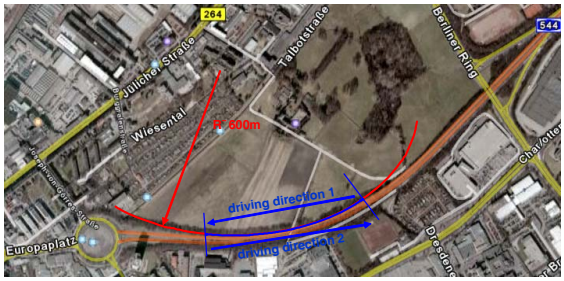

Figure 17. Curved highway segment.

The measurement duration is 20 s and the distance between the vehicles is 15 m. The measurement data show positive values for the curvature in a range of 0.00167 m^{-1}. Hence the model output can be considered as correct.

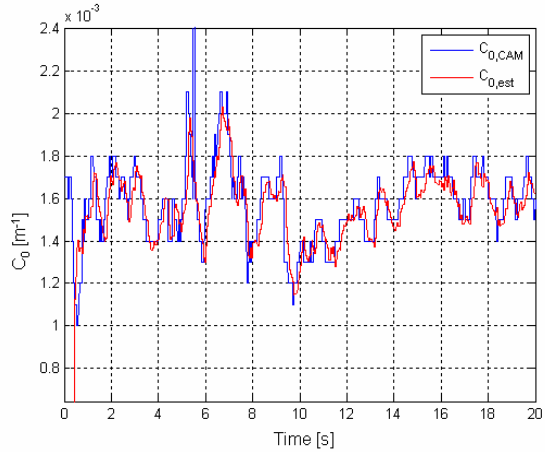

Figure 18. Measurement results for curvature $C_{0,CAM}$ and $C_{0,est}$.

Between 5 and 6 s the camera delivers wrong measurement values for the curvature. The street model compensates this and delivers correct values because the wrong measurement values are detected by a gating function (not described in this paper) and are not feed into the street model.
With the help of the curvature signal from the target vehicle and the implemented street model, a statement about the change of curvature is possible. The upper diagram in Figure 19 shows the curvature signal in the target vehicle, the lower shows the model based curvature change. Here no reference value was available but an estimation can be done with Equation (23). Using the curvature in the target vehicle e.g. at 18 s ($1.4 \cdot 10^{-3}$ m^{-1}) and the curvature in the ego-vehicle at 18 s ($1.6 \cdot 10^{-3}$ m^{-1}) as well as the model based curvature change ($1.3 \cdot 10^{-5}$ m^{-2}) in Equation (23), the resulting distance is 15.4 m, which is close to the distance between the trucks in the test (15 m). Hence the values for the curvature change can be considered as reliable.

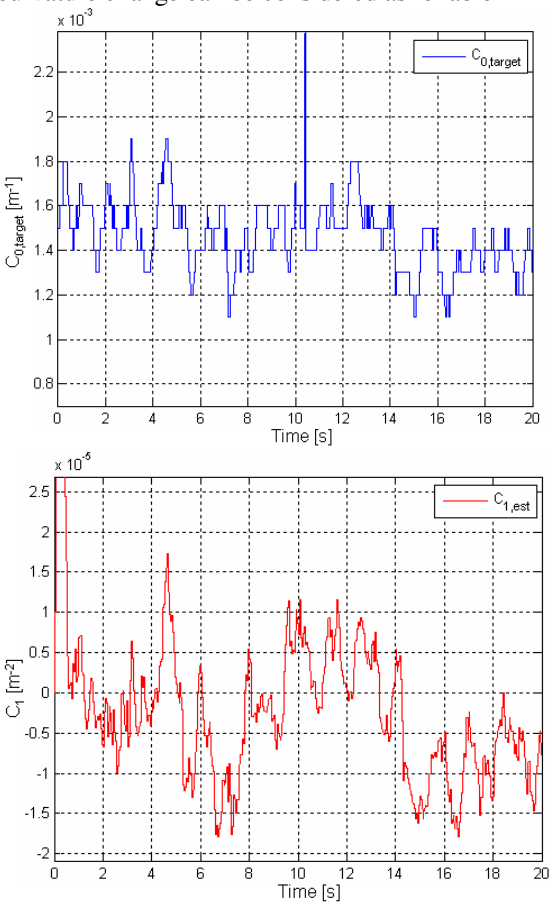

Figure 19. Curvature signal of target vehicle (above) and estimated change of curvature (below).

As stated above, the knowledge about the position of the target vehicle in the IDIS lidar sensor coordinate system can be used to determine a curvature C^*_0. Figure 20 shows the results of this approach with the curvature calculated from the target vehicle position (blue) and the curvature from the street model (red) for a test drive into direction 1 (negative curvature) with 80 kph and 30 m distance between the vehicles.

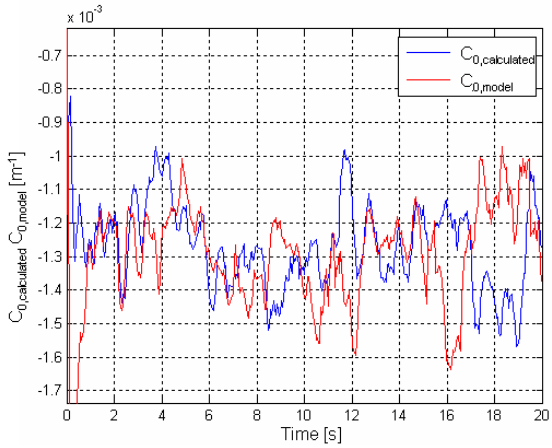

Figure 20. Results of the corrected curveature estimation.

After the Kalman-Filter is engaged both curvatures show comparable values, delivering a redundant signal for the curvature which can be used later in the CM system development.

Driving tests for the determination of the quality of GPS based distance measurement

Having checked the funciotnality of the models, in a next step the accuracy of the GPS and communication based positioning is investigated. Therefore the test drives on highways are examined as a first step. With the help of offline simulations performed with the highway test data, the threshold values of the object detection algorithm are tuned.
In order to give a statement about the quality of this approach for the detection of standing objects, test drives on ika's test track with a static target vehicle are executed in a second step. The results of both experiments are presented in the following.

Highway tests – The following diagrams show the relative position of the target vehicle with respect to the ego-vehicle as a function of time (red graphs are the measured data of the IDIS sensor and blue graphs show the communication based position data).
The test drive depicted in Figure 21 shows an approaching maneuvre of the ego-vehicle towards the target vehicle with a starting distance of about 97 m and a relative velocity of about 7 kph. Examining both diagrams, the influence of GPS data updates can be seen (the graphs show a step). Furthermore, in the upper diagram a signal dropout at the time of 11 s (blue graph) is remarkable. This is due to a short break down of the C2C, so that the GK coordinates of the target vehicle are not updated. The lower diagram shows that a break down of the C2C

communication affects the lateral positioning not as much as the longitudinal position due to the higher velocity in longitudinal direction.
In order to acquire robust data even if C2C breaks down, a further Kalman-Filter based vehicle model of the target vehicle could be implemented in the ego-vehicle. Thus, in case of communication break down, the position of the target vehicle could be estimated model based.

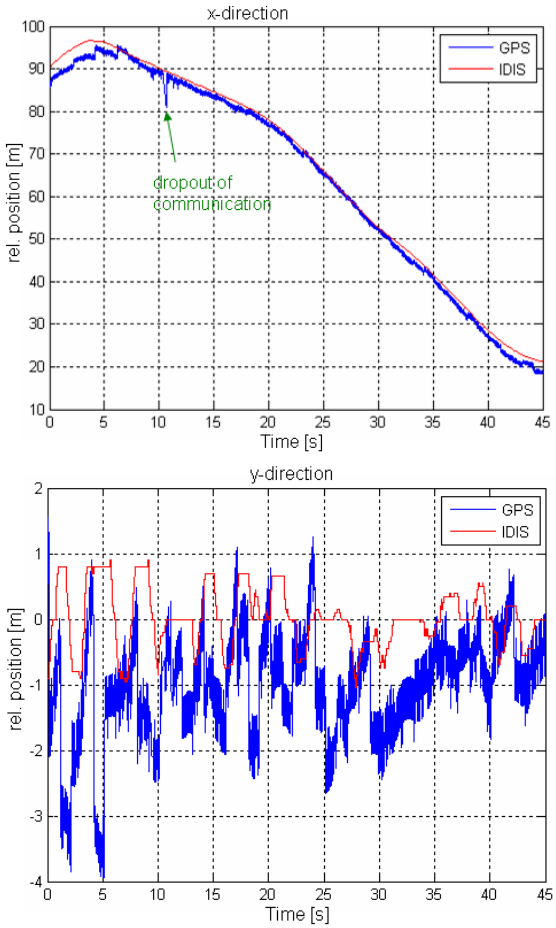

Figure 21. Relative localisation GPS- and IDIS based.

If the dropout from communication break down is neglected, the maximum difference between IDIS- and communication data is -2.5 m (mean value: -1.5 m) in longitudinal direction. For the lateral direction the positioning accuracy is less. At the time of 5 s the difference is -4.8 m.
Figure 22 shows two diagrams for the relative position of the target vehicle, too. Within this test a constant distance of 55 m between ego- and target vehicle was held. The positioning accuracy in lateral direction (lower diagram) did not change in comparison to the measurement described above. In contrast, in longitudinal direction a larger difference is shown. The maximum difference between the IDIS- and the communication based signal is +6.9 m (mean value: +4.85 m).
The result of the executed test drives is that the quality of the GPS based positioning is depending on various and hard to determine factors. For example, 40 % of the test drives were executed having a clear sky while 60 % of the test drives were executed when it was clouded. Within the experiments with a clear sky (e.g. the test drive in Figure 21) the measurement results are better than the experiments when it was cloudy (e.g. test drive in Figure 22) what can be caused by a better satellite reception. A further factor to the quality of the positioning accuracy is the current satellite constellation ("bad geometry") [7].
Having analysed the measurement results for the test drives, two of five thresholds for the signal differences of the redundant signals are determined (distance in longitudinal/lateral direction).
In order to determine the remaining three thresholds (difference of velocity-, acceleration- and vehicle width signal) further simulations are carried out. Therefore the recorded sensor signals are fed in the object detection algorithm and the thresholds are varied. The effects of the threshold variation is evaluated by the help of a tool that shows the recorded scene with a birds eye view (see Figure 23).

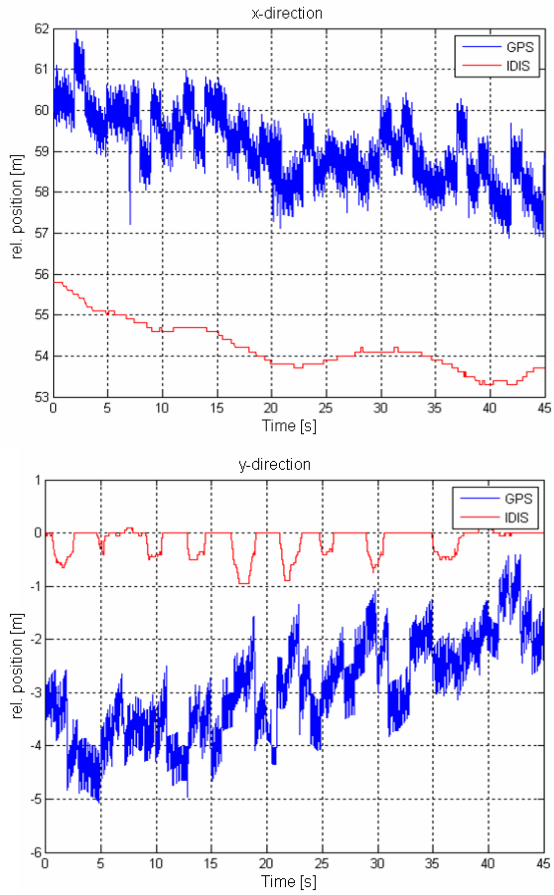

Figure 22. Relative localisation GPS- and IDIS based.

Displayed signals are the estimated lane trajectory of the street model as well as the lane trajectory corrected with communication data from target vehicle (red and blue graph in Figure 23). The direction of the vehicle in lane is indicated by the

yellow line starting from the origin of the coordinate system. Furthermore, the IDIS data (in Figure 23 depicted as different symbols in the colours red and cyan) and the GPS and communication based position of the target vehicle (magenta coloured square) are displayed.

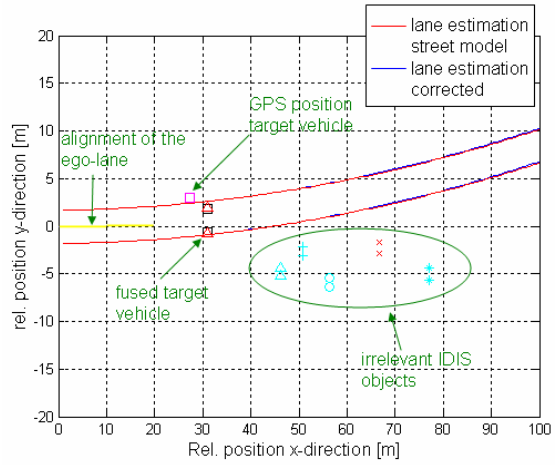

Figure 23. Tool for test drive evaluation.

If a relevant target is detected by the algorithm, it is marked as a black square in the bird's eye tool.
The simulations are run with different threshold constellations and the effects are observed in the evaluation tool. With this process the thresholds are determined.
One situation shown in Figure 24 could be critical for the determination of the target vehicle.

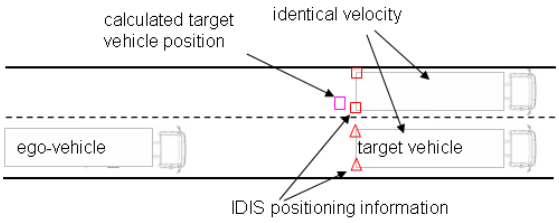

Figure 24. Critical situation for data fusion.

In this situation two vehicles with the identical width and velocity drive next to each other with the same distance towards the ego vehicle. The calculated position of the target vehicle differs from the position measured by the IDIS sensor. While the width, velocity, acceleration and the longitudinal distance of the two preceding vehicles is identical, the lateral position of the calculated point is different. The lateral position is located closer to the vehicle driving in the left lane. If both vehicles are equipped with a communication system, they will transmit their lane numbers to the ego-vehicle. Thus, the vehicle driving in the left lane can be regarded as not relevant by the object detection and the correct vehicle will be found.

Tests with target vehicle standing still – These experiments are executed on the test track of ika and can indentify possible factors that influence the quality of the communication based detection and ranging. Therefore two experiments were carried out with 34 measurements on two different days under different weather conditions. The procedure is shown in Figure 25.

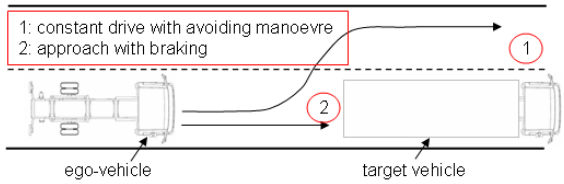

Figure 25. Experiment procedure.

Within experiment 1 the ego-vehicle approaches with velocities of 20, 40, 50, 60, 70 and 75 kph to the rear of the target vehicle. The ego-vehicle avoids the collision at a very late moment by steering. In the second experiment the ego-vehicle approaches with velocities of 20, 40, 50, 60 and 70 kph to the rear of the target vehicle, braking heavily at a late moment and comming to standstill behind the target vehicle.
The upper diagram in Figure 26 shows the evaluation of a test drive of the first experiment with a velocity of 50 kph. In this diagram the IDIS distance signal (red) and the calculated communication based distance (blue) are plotted as a function of the time. It is obvious that the IDIS sensor does not detect the target vehicle anymore starting from a distance of 20 m because the target passes out of the sensor detection range due to the emergency steering manoevre. In contrast, the GPS delivers distance information continuously. The difference between IDIS- and GPS based distance signal is almost constantly (7.5 m). If all test drives of experiment 1 are considered it is noticeable that the difference in the distance signal changes with the relative velocity.
In order to point out the influence of the relative velocity, the mean distance failure of different test drives for the two different test days is depicted in the lower diagram of Figure 26 as a function of the relative velocity.

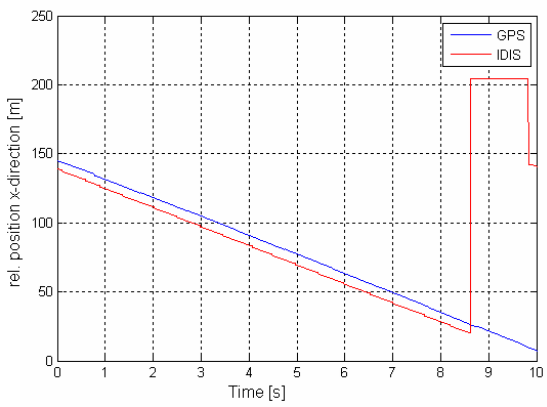

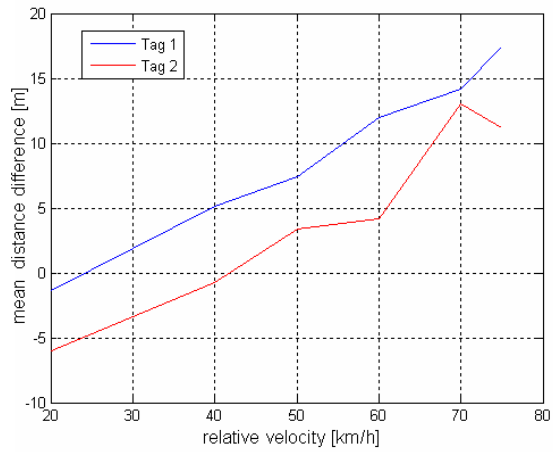

Figure 26. Measurement evaluation of experiment 1 (above) and mean distance failure as a function of the relative velocity (below).

Due to the seperated graphs of the tests it is obvious that the mean distance error of the first day is always larger than the error of day two. This error might be a result from different satellite constellations and different weather conditions. Furthermore, the distance error rises with increasing relative velocity.
Accordingly, the data of experiment 2 confirm the dependence of the quality of the communication based detection and ranging. Figure 27 shows the evaluation of the second test procedure with a starting ego-vehicle velocity of 70 kph. The process of the velocity signal is given by the green line in Figure 27. If the velocity decreases, the distance failure decreases, too. This proves the relative velocity dependency.

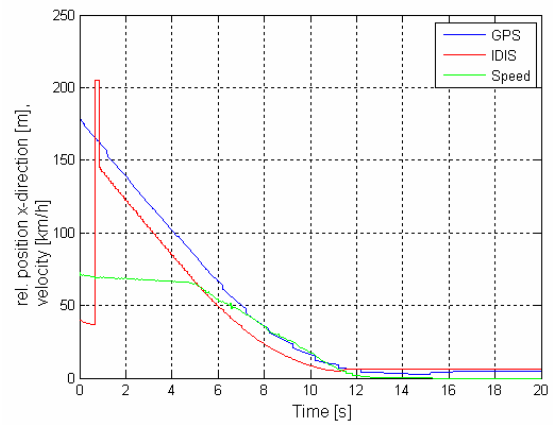

Figure 27. Measurement evaluation of experiment 2.

The applicability of this approach for the validation of objects standing still is hence depending of the occuring relative velocities. In the executed experiments, the developed algorithm delivered promising results up to a relative velocity of 50 kph (day one) resp. 60 kph (day two). Above this relative velocities the developed algorithm was not able to deliver dependable results due to the high difference of calculated and IDIS positioning data.

CONCLUSION

The described system delivers robust input data for the development of collision warning (CW) and collision mitigation (CM) systems.
Therefore a GPS-Tracking was implemented, delivering a higher update rate for the vehicle position in GK coordinates. With the use of C2C, the GK coordinates and further vehicle relevant data from the preceding vehicle are transferred to the following vehicle. The run of the road trajectory is determined by ego-vehicle data and data from preceding vehicle also transmitted via C2C.
The GK coordinates from the preceding vehicle are used to determine its relative position to the ego vehicle. These data are used together with further vehicle data for the determination of the relevant target out of the data from an IDIS Lidar sensor in order to get a robust detection of stationary targets.
Within driving tests and simulations (data gained from these driving tests), the function of the detection system was tuned. It can be stated that the used concept with environmental sensors, GPS and C2C is generally suitable for the detection of stationary targets. On the other hand some limitations from the used setup and hardware must be mentioned. These limitations refer to the relative velocity between the stationary target and ego-vehicle. Within the tests a dependency of the relative velocity to the communication based position determination was found. Furthermore, the accuracy of GPS data is depending on the weather, number of satellites and satellite constellation. For future developments a DGPS system with higher accuracy should be used and a synchronisation of the C2C communication should be implemented.
Further improvements could be achieved by implementation of a bicycle model into the GPS-tracking function and the determination of a reference velocity, weighting the signals from front and rear axle speed sensors during acceleration or braking.
Despite the mentioned limitations, the presented concept was used within a CW- and CM system on the test track with promission results in [8] and we will continue the work on this topic in order to contribute to an accident reduction one day.

REFERENCES

[1] Ellinghaus, D.; Steinbrecher, J. 2002. “Lkw im Straßenverkehr“. Eine Untersuchung über die Beziehung zwischen Lkw und Pkw-Fahrern. Uniroyal Verkehrsuntersuchung im Auftrag der Continental AG. Hannover

[2] Langwieder, K.; Knoll, P. 2006. „Der Sicherheitsaspekt in Realunfällen – Überlegungen z. volkswirtschaftlichen Nutzen von prädiktiven Fahrerassistenzsystemen“. EUROFORUM Congress

[3] Genzel, M.; Padron, J. 2005. “Adaptive Cruise Control“. Autonome Fahrzeuge Seminar. Freie Universität Berlin

[4] Southall, B.; Taylor, C. 2000. “Stochastic road shape estimation”. GRASP Laboratory, University of Pennsylvania, Philadelphia, PA 19104. www.cis.udel.edu/~cer/arv/readings/paper_southall.pdf, called: 26.03.08. Philadelphia, USA

[5] RAS-L-1 1995. “Richtlinien für die Anlage von Straßen RAS Teil: Linienführung RAS-L”. Forschungsgesellschaft für Straßen- und Verkehrswesen. Cologne, Germany

[6] Föllinger, O. 1990. “Regelungstechnik: Einführung in die Methoden und ihre Anwendung”. Hüthig, Heidelberg 1990

[7] Bozkurt, F. 2008. “Development and integration of a digital card module into a sensor fusion system”. Mini Thesis, ika - Institut für Kraftfahrzeuge Aachen, RWTH Aachen University, Aachen, Germany

[8] Wimmershoff, M. 2008. “Aufbau eines kommunikations- und umfeldsensorbasierten Collision Mitigation Systems für Nutzfahrzeuge”. Master Thesis, ika - Institut für Kraftfahrzeuge Aachen, RWTH Aachen University”, Aachen, Germany